Available online at www.sciencedirect.com
ScienceDirect
International Communications in Heat and Mass Transfer 34 (2007) 1017–1029
International Communications in HEAT and MASS TRANSFER
www.elsevier.com/locate/ichmt

The effects of Ohmic heating and viscous dissipation on unsteady MHD and slip flow over a porous rotating disk with variable properties in the presence of Hall and ion-slip currents ☆

Emmanuel Osalusi *, Jonathan Side, Robert Harris

Renewable Energy Group, International Centre for Island Technology (ICIT), Institute of Petroleum Engineering, Heriot-Watt University, Old Academy, Back Road, Stromness, Orkney KW16 3AW, Scotland, United Kingdom

Available online 14 June 2007

Abstract

The effects of Ohmic heating and viscous dissipation on unsteady laminar magneto-hydrodynamics (MHD) flow of a viscous Newtonian and electrically conducting fluid over a rotating disk taken into account the variable fluid properties (density, (ρ), viscosity, (μ) and thermal conductivity, (κ)) in the presence of Hall and ion-slip currents effects have been examined. These fluid properties are taken to be dependent on temperature. The unsteady Navier–Stokes equations along with the energy equation are reduced to a system of ordinary differential equations by using similarity transformations and the resulting equation system is solved numerically by using a shooting method. Results for the details of the velocity as well as temperature are shown graphically and the numerical values of the skin friction and the rate of heat transfer are entered in tables.

Keywords: Rotating disk; Ohmic heating; Viscous dissipation; Shooting method

1. Introduction

The study of flow and (or) heat and mass transfer over rotating bodies is of considerable interest due its occurrence in many industrial, geothermal, geophysical, technological and engineering applications. Such a study is important in the design of turbines (gas or marine) and turbo-machines, in estimating the flight path of rotating wheels and spin-stabilized missiles and in the modeling of many geophysical vortices.

The hydrodynamic flow due to an infinite rotating disk was first introduced by von Karman [1]. He formulated the problem in the steady state and used similarity transformations to reduce the governing partial differential equations to ordinary differential equations. Asymptotic solutions were obtained for the reduced system of ordinary differential equations [2]. The extension of the steady hydrodynamic problem to the transient state was done by Benton [3]. The influence of an external uniform magnetic field on the flow due to a rotating disk was studied [4] without considering the Hall effect. More applications can be found in [5–7].

☆ Communicated by W.J. Minkowycz.

* Corresponding author.
E-mail address: eo26@hw.ac.uk (E. Osalusi).

0735-1933/$ - see front matter © 2007 Elsevier Ltd. All rights reserved.
doi:10.1016/j.icheatmasstransfer.2007.05.009

Nomenclature

u	radial velocity, m/s
P	pressure, N/m^2
g	gravitational acceleration, m/s^2
L	characteristic length, m
w	axial velocity, m/s
Nu	Nusselt number
T	fluid temperature, K
B_0	magnetic flux density
c_p	specific heat at constant temperature, J kg^{-1} K^{-1}
Pr	Prandlt number, $=\mu_0 c_p/k_0$
T_w	wall temperature, °C
M	magnetic interaction parameter, $=\sigma B_0^2/(\rho_0\Omega)$
W	uniform suction/injection, $= w/\sqrt{v_0\Omega}$
U_t	target velocity, m/s
v	tangential velocity, m/s
r	radial axis, m
z	vertical axis, m
Kn	Knudsen number
Re	Reynolds number, $=\Omega r^2/v_0$
Re_m	magnetic Reynolds number
n	normal direction to the wall

Greek symbols

v_0	uniform kinematic viscosity, m^2/s
δ	unsteadiness parameter
ϕ	vertical angle of the disk
η	normal distance from the disk, $=z(\Omega/v_0)^{1/2}$
Ω	angular velocity, m/s
μ	dynamic viscosity, N s/m^2
κ	thermal conductivity coefficient
ρ	fluid density, kg/m^3
σ	electrical conductivity
$\sigma*$	Stefan–Boltzmann constant
$\kappa*$	absorption coefficient
ε	relative temperature different parameter, $=\triangle T/T_0$
v	kinematic viscosity, m^2/s
η	dimensional normal distance
τ_t	tangential skin friction
τ_r	radial skin friction
ψ	target momentum accommodation coefficient
γ	slip factor, $[(2-\psi)\lambda\Omega^{1/2}]/[\psi v^{1/2}]$

Subscripts

i	initial condition
w	condition of the wall
0	condition at free stream

Attia et al. [8] studied the steady hydro-magnetic problem taking the Hall effect into consideration. Later Attia [9] extended the problem to include the effect of uniform suction or injection on the flow of a conducting fluid due to a rotating disk considering the Hall and ion-slip current with the neglect of viscous dissipation. Several authors ([10–40]) had shown that viscous dissipation effect plays an important role in natural convection in various devices that are subjected to large deceleration, or which operate at high rotative speeds that are also in strong gravitational field processes on large scales and geological process. Hence the motivation behind this study.

A completely different extension of von Karmanos one-disk problem is the analysis of Sparrow et al. [10]. They considered the flow of a Newtonian fluid due to the rotation of a porous-surfaced disk and for that purpose replaced the conventional no-slip boundary conditions at the disk surface with a set of linear slip-flow conditions. A substantial reduction in torque then occurred as a result of surface slip. This problem was recently reconsidered by Miklavcic and Wang [11] who pointed out that the same slip-flow boundary conditions as those used by Sparrow et al. [10] also could be used for slightly rarefied gases or for flow over grooved surfaces.

This paper deals with the effects of Ohmic heating and viscous dissipation on unsteady flow over an infinitely disk with slip boundary which is rotating with time-dependent angular velocity in the presence of Hall and ion-slip currents. The fluid is electrically conducting with variable properties. The magnetic field is applied normal to the disk surface. The Navier–Stokes equations and the energy equation governing the unsteady flow admit a self-similar solution proposed by von Karman [1] if the angular velocity of the disk and the magnetic field square vary inversely as a linear function of time. The resulting differential equation system is solved numerically by the shooting method (Osalusi and Sibanda [12]). In the following sections, the problem is formulated, analyzed and discussed.

2. Governing equation

The description of the physical problem closely follows that of Osalusi and Sibanda [12]. We use a non-rotating cylindrical polar coordinate system, (r, φ, z) where z is the vertical axis in the cylindrical coordinates system with r and φ as the radial and tangential axes respectively. The homogeneous, electrically conducting fluid occupies the region $z>0$ with the rotating disk placed at $z=0$ and rotating with a time-dependent angular velocity Ω which varies inversely as a linear function of time (i.e., $\Omega=\Omega_0(1-\delta t*)^{-1}$), $\delta t*<1$). The fluid velocity components are (u, v, w) in the directions of increasing (r, φ, z) respectively, the pressure is P, the density of the fluid is ρ and T is the fluid temperature. The surface of the rotating disk is maintained at a uniform temperature T_w. Far away from the wall, the free stream is kept at a constant temperature T_0 and at constant pressure P_0.

An external strong magnetic is applied in the z-direction and has a constant flux density B_0. The magnetic Reynolds number of the flow is taken to be small enough so that the induced distortion of the applied magnetic field can be neglected. The electron–atom collision frequency is assumed to be relatively high, so that the Hall and ion-slip effects cannot be neglected. Assuming the disk to be electrically non-conducting, the generalized Ohm's law gives $j_z=0$ everywhere in the flow. The governing equations for this investigation are modified to include viscous and Ohmic heating effects with the generalized Ohm's and Maxwell's laws.

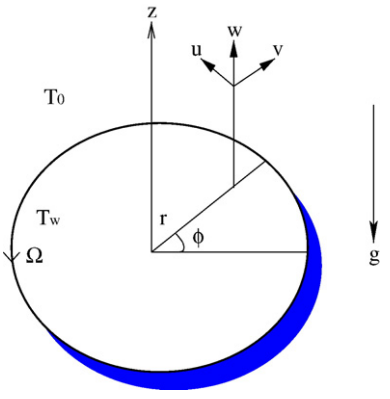

Fig. 1. The flow configuration and the coordinate system.

Following Jayaraj [30] (and more recently, Maleque and Sattar [20], Osalusi and Sibanda [12]), we assume that the dependency of the fluid properties, viscosity (μ) and thermal conductivity coefficients (κ) and density (ρ) are functions of temperature alone and obey the following laws;

$$\mu = \mu_0[T/T_0]^a, \quad \kappa = \kappa_0[T/T_0]^b, \quad \rho = \rho_0[T/T_0]^c, \tag{1}$$

where a, b and c are arbitrary exponents, κ_0 is a uniform thermal conductivity of heat, and μ_0 is a uniform viscosity of the fluid. As in Osalusi and Sibanda [12] the fluid under consideration is a flue gas with $a=0.7$, $b=0.83$, and $c=-1.0$. The case $c=-1.0$ is that of an ideal gas. The physical model and geometrical coordinates are shown in Fig. 1. The equations governing the motion of the unsteady MHD laminar flow of the homogeneous fluid take the following form

$$\frac{\partial}{\partial r}(pru) + \frac{\partial}{\partial z}(prw) = 0, \tag{2}$$

$$\rho\left(\frac{\partial u}{\partial t} + u\frac{\partial u}{\partial r} - \frac{v^2}{r} + w\frac{\partial u}{\partial z}\right) + \frac{\partial P}{\partial r} = \frac{\partial}{\partial r}\left(\mu\frac{\partial u}{\partial r}\right) + \frac{\partial}{\partial r}\left(\mu\frac{u}{r}\right) + \frac{\partial}{\partial z}\left(\mu\frac{\partial u}{\partial z}\right) - \frac{\sigma B_0^2}{\left(\alpha^2+\beta_e^2\right)}(\alpha u - \beta_e v), \tag{3}$$

$$\rho\left(\frac{\partial v}{\partial t} + u\frac{\partial v}{\partial r} - \frac{uv}{r} + w\frac{\partial v}{\partial z}\right) = \frac{\partial}{\partial r}\left(\mu\frac{\partial v}{\partial r}\right) + \frac{\partial}{\partial r}\left(\mu\frac{v}{r}\right) + \frac{\partial}{\partial z}\left(\mu\frac{\partial v}{\partial z}\right) - \frac{\sigma B_0^2}{\left(\alpha^2+\beta_e^2\right)}(\alpha v + \beta_e u), \tag{4}$$

$$\rho\left(\frac{\partial w}{\partial t} + u\frac{\partial w}{\partial r} + w\frac{\partial w}{\partial z}\right) + \frac{\partial P}{\partial z} = \frac{\partial}{\partial r}\left(\mu\frac{\partial w}{\partial r}\right) + \frac{1}{r}\frac{\partial}{\partial r}(\mu w) + \frac{\partial}{\partial z}\left(\mu\frac{\partial w}{\partial z}\right), \tag{5}$$

$$\rho c_p\left(\frac{\partial T}{\partial t} + u\frac{\partial T}{\partial r} + w\frac{\partial T}{\partial z}\right) = \frac{\partial}{\partial r}\left(\kappa\frac{\partial T}{\partial r}\right) + \frac{\kappa}{r}\frac{\partial T}{\partial r} + \frac{\partial}{\partial z}\left(\kappa\frac{\partial T}{\partial z}\right) + \frac{\sigma B_0^2}{\left(\alpha^2+\beta_e^2\right)}\left(u^2+v^2\right) + \mu\left[\left(\frac{\partial u}{\partial z}\right)^2 + \left(\frac{\partial v}{\partial z}\right)^2\right], \tag{6}$$

where, σ $(=(e^2 n_e t_e)/m_e)$ is the electrical conductivity, e is the electron charge, t_e is the electron collision time, n_e is the electron number density, and m_e is the mass of the electron. c_p and t are the specific heat at constant pressure of the fluid and time respectively. $\alpha=1+\beta_i\beta_e$, β_e $(=\omega_e t_e)$ is the Hall parameter with ω_e $(=eB_0/m_e)$ as the electron frequency, and β_i $(=en_eB_0/((1+n_e/n_a)K_{ai}))$ as the ion-slip parameter, n_a as the neutral particle number density, and K_{ai} as the friction coefficient between ions and neutral particles. The fourth and fifth terms on the RHS of Eq. (6) denote the magnetic and viscous heating terms, respectively.

When the mean free path of the fluid particles is comparable to the characteristic dimensions of the flow field domain, Navier–Stokes equations break down since the assumption of continuum media fails. In the range $0.1<Kn<10$ of Knudsen number, the high order continuum equations, e.g. Burnett equations should be used. For the range of $0.1<Kn<10.001$, no-slip boundary conditions cannot be used and should be replaced with the following expression (Gad-el-Hak [25]):

$$U_t = \frac{2-\psi}{\psi}\lambda\frac{\partial U_t}{\partial n} \tag{7}$$

where U_t is the target velocity, n is the normal direction to the wall, ψ is the target momentum accommodation coefficient and λ is the mean free path. For $Kn<0.001$, the no-slip boundary condition is valid, therefore, the velocity

Table 1
Comparison of current and recent numerical values of the radial and tangential skin-friction coefficients and the rate of heat transfer coefficient obtained for $Pr=0.71$, M≃0, γ≃0δ≃0, Ec≃0, and $\varepsilon=0$

W	Present			Osalusi and Sibanda [12] (M≃0)			Maleque and Sattar [20]		
	$F'(0)$	$-G'(0)$	$-\theta'(0)$	$F'(0)$	$-G'(0)$	$-\theta'(0)$	$F'(0)$	$-G'(0)$	$-\theta'(0)$
0	0.42406	0.65140	0.53873	0.42406	0.65140	0.53873	0.51015	0.61596	0.32576
−2	0.23239	2.06872	1.51962	0.23239	2.06872	1.51962	0.24251	2.03911	1.44212
−4	0.12462	4.00649	2.85201	0.12462	4.00649	2.85201	0.12477	4.00537	2.84470
−5	0.09990	5.00289	3.55414	0.09990	5.00289	3.55414	0.09996	5.00297	3.55411
−10	0.04999	10.00033	7.10016	0.04999	10.00033	7.10016	0.05059	10.00156	7.1020

at the surface is equal to zero. In this study the slip and the no-slip regimes of the Knudsen number that lies in the range $0.1>Kn>0$ is considered. By using Eq. (7), the boundary conditions are introduced [5] as follows:

$$\begin{aligned} &u(t,r,0)=\frac{2-\psi}{\psi}\lambda\frac{\partial u}{\partial z},\quad v(t,r,0)=r\Omega+\frac{2-\psi}{\psi}\lambda\frac{\partial v}{\partial z},\quad w(t,r,0)=W,\quad T(t,r,0)=T_{\mathrm{w}},\\ &u(t,r,\infty)=0,\qquad v(t,r,\infty)=0,\quad T(t,r,\infty)=T_{\mathrm{w}},\qquad P(t,r,\infty)=0. \end{aligned} \tag{8}$$

The initial conditions are given by

$$\begin{aligned} &u(0,r,z)=u_{\mathrm{i}}(r,z),\quad v(0,r,z)=v_{\mathrm{i}}(r,z),\quad w(0,r,z)=w_{\mathrm{i}}(r,z),\\ &T(0,r,z)=T_{\mathrm{i}}(r,z),\quad P(0,r,z)=P_{\mathrm{i}}(r,z). \end{aligned} \tag{9}$$

3. Similarity transformation

If the angular velocity of the disk Ω and the magnetic field square B^2 vary inversely as a linear function of time (i.e., $\Omega=\Omega_0(1-\delta t^*)^{-1}$, $B^2=B_0^2(1-\delta t^*)^{-1}$) then the partial different equations (Eqs. (2)–(6)) can be reduced to a system of ordinary differential equations provided we apply the following transformations:

$$\begin{aligned} &\eta=z(\Omega_0/v_0)^{1/2}(1-\delta t^*)^{-1/2},\quad t^*=\Omega_0 t,\qquad \delta t^*<1,\qquad \Omega=\Omega_0(1-\delta t^*)^{-1},\\ &u=r\Omega_0(1-\delta t^*)^{-1}F(\eta),\qquad v=r\Omega_0(1-\delta t^*)^{-1}G(\eta),\quad w=(v_0\Omega_0)^{1/2}(1-\delta t^*)^{-1}H(\eta),\\ &B^2=B_0^2(1-\delta t^*)^{-1},\qquad T-T_0=(T_{\mathrm{w}}-T_0)\theta(\eta), \end{aligned} \tag{10}$$

where v_0 is a uniform kinematic viscosity of the fluid. Substituting these transformations into Eqs. (2)–(6) gives the nonlinear ordinary differential equations,

$$H'+2F+cH\theta'(1+\theta)^{-1}=0, \tag{11}$$

$$F''+a(1+\theta)^{-1}\theta'F'-\left[\frac{\delta\eta}{2}F'+\delta F+F^2-G^2+HF'\right](1+\theta)^{c-a}-\left[\frac{M}{(\alpha^2+\beta_{\mathrm{e}}^2)}(\alpha F-\beta_{\mathrm{e}}G)\right](1+\theta)^{-a}=0, \tag{12}$$

$$G''+aG'\theta'(1+\theta)^{-1}-\left[\frac{\delta\eta}{2}G'+\delta G+2FG+HG'\right](1+\theta)^{c-a}-\left[\frac{M}{(\alpha^2+\beta_{\mathrm{e}}^2)}(\alpha G+\beta_{\mathrm{e}}F)\right](1+\theta)^{-a}=0, \tag{13}$$

$$\theta''+b\theta'^2(1+\theta)^{-1}+Pr(1+\theta)^{-b}\left[-\left(\frac{\delta\eta}{2}\theta'+H\theta'\right)(1+\theta)^{c}+\frac{EcM}{\alpha^2+\beta_{\mathrm{e}}^2}\left(F^2+G^2\right)+Ec\left(F'^2+G'^2\right)(1+\theta)^{a}\right]=0, \tag{14}$$

Table 2
Numerical values of $F'(0)$, $-G'(0)$ and $\theta'(0)$ for various values of γ, δ, M, Ec, β_e and β_i with $Pr=0.72$, $W=-1$ and $\varepsilon=0.1$

γ	δ	M	Ec	β_e	β_i	$F'(0)$	$-G'(0)$	$-\theta'(0)$
0.0	0.3	1.0	0.3	0.1	0.2	0.193138806478034	1.803140085716445	1.064510561913337
0.1	0.3	1.0	0.3	0.1	0.2	0.120228739205813	1.529770723179624	1.125650907360875
0.2	0.3	1.0	0.3	0.1	0.2	0.080371406904560	1.326738027162156	1.163568054530476
0.3	0.3	1.0	0.3	0.1	0.2	0.056673631135413	1.170875838852254	1.188634404531857
0.4	0.3	1.0	0.3	0.1	0.2	0.041645662991824	1.047699397550310	1.206052988007736
0.1	0.0	1.0	0.3	0.1	0.2	0.124392583426896	1.492242900023453	1.144533949512801
0.1	1.0	1.0	0.3	0.1	0.2	0.111309979935868	1.614087434436402	1.081533332848297
0.1	2.0	1.0	0.3	0.1	0.2	0.100262945995988	1.727179817887927	1.018550150112623
0.1	3.0	1.0	0.3	0.1	0.2	0.090881670215205	1.832398990308442	0.955884766711371
0.1	4.0	1.0	0.3	0.1	0.2	0.082867639122694	1.930542587651596	0.893812891976242
0.1	0.3	0.0	0.3	0.1	0.2	0.124412197047097	1.327440404265739	1.162467815015826
0.1	0.3	0.1	0.3	0.1	0.2	0.123892990581756	1.349144124680710	1.158425121244849
0.1	0.3	0.2	0.3	0.1	0.2	0.123399819984110	1.370495561559215	1.154470038063887
0.1	0.3	0.3	0.3	0.1	0.2	0.122931158279043	1.391504919151914	1.150599573985529
0.1	0.3	0.4	0.3	0.1	0.2	0.122485587008875	1.412182007226904	1.146810871092867
0.1	0.3	1.0	0.0	0.1	0.2	0.120358521689586	1.52918082164352	1.27852759756793
0.1	0.3	1.0	1.0	0.1	0.2	0.119927385511534	1.53114513263402	0.76859118441600
0.1	0.3	1.0	2.0	0.1	0.2	0.119500422533550	1.53310365835521	0.25766562762458
0.1	0.3	1.0	3.0	0.1	0.2	0.119077565918557	1.53505642322928	−0.25424283684431
0.1	0.3	1.0	4.0	0.1	0.2	0.118658752387180	1.53700345975536	−0.76712806748436
0.1	0.3	1.0	0.3	0.0	0.2	0.101551710778315	1.532602444666924	1.123499018570219
0.1	0.3	1.0	0.3	0.1	0.2	0.120228739205813	1.529770723179625	1.125650907360876
0.1	0.3	1.0	0.3	0.2	0.2	0.137045643720214	1.523996094681857	1.128170437011460
0.1	0.3	1.0	0.3	0.3	0.2	0.151559523028782	1.516026885632672	1.130884532623709
0.1	0.3	1.0	0.3	0.4	0.2	0.163620531565223	1.506618859115845	1.133643920376162
0.1	0.3	1.0	0.3	0.1	0.0	0.120532677835399	1.533497120190081	1.124457800044671
0.1	0.3	1.0	0.3	0.1	0.1	0.120377617028435	1.531617085902095	1.125062136205699
0.1	0.3	1.0	0.3	0.1	0.2	0.120228739205813	1.529770723179625	1.125650907360876
0.1	0.3	1.0	0.3	0.1	0.3	0.120085789593005	1.527957143887828	1.126224655432954
0.1	0.3	1.0	0.3	0.1	0.4	0.119948525515631	1.526175490560005	1.126783898766315

where, $Pr=\mu_0 c_p/k_0$ is the Prandtl number, $M=\sigma B^2/(\rho_0\Omega_0)$ is the magnetic interaction parameter that represents the ratio of the magnetic force to the fluid inertial, $Ec=(r^2\ \Omega^2)/(\Omega_0\ \Delta T c_p)$ is the Eckert number and $\varepsilon=\Delta T/T_0$ is the relative temperature difference parameter, which is positive for heated surface, negative for a cooled surface and zero for uniform properties. A prime symbol denotes a derivative with respect to η. The transformed boundary conditions are given by;

$$F=\gamma F',\quad G=1+\gamma G',\quad H=W,\quad \theta=1,\quad \text{at}\ \eta=0 \tag{15}$$

$$F=G=\theta=p=0,\ \text{at}\ \eta\rightarrow\infty, \tag{16}$$

where $\gamma=[(2-\psi)\lambda\Omega^{1/2}]/[\psi\nu^{1/2}]$ is the slip factor, $W=w/\sqrt{v_0\Omega}$ represents a uniform suction ($W<0$) or injection ($W>0$) at the surface. The boundary conditions (16) imply that both the radial (F), the tangential (G), temperature, concentration and pressure vanish sufficiently far away from the rotating disk, whereas the axial velocity component (H) is anticipated to approach a yet unknown asymptotic limit for sufficiently large η-values.

The skin-friction coefficients and the rate of heat transfer to the surface are given by the Newtonian formulas:

$$\tau_t=\left[\mu\left(\frac{\partial v}{\partial z}+\frac{1}{r}\frac{\partial w}{\partial\phi}\right)\right]_{z=0}=\mu_0(1+\ )^a R_e^{\frac{1}{2}}\Omega G'(0),$$

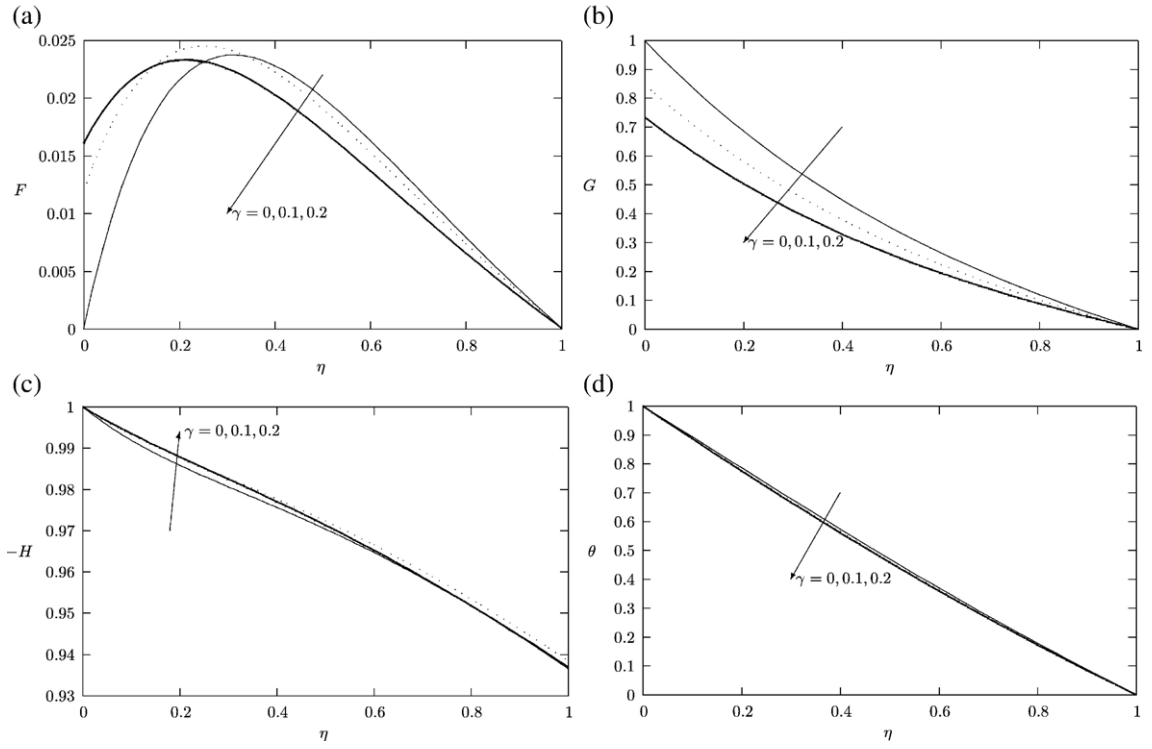

Fig. 2. (a) Effect of γ on the radial velocity profiles and (b) effect of γ on the tangential velocity profiles: for Ec=0.3, Pr=0.72, ε=0.1, β_e=0.1, β_i=0.2, M=1, δ=0.3 and W=−1. (c) Effect of γ on the axial velocity profiles and (d) effect of γ on the temperature profiles: for Ec=0.3, Pr=0.72, β_e=0.1, β_i=0.2, M=1, δ=0.3 and W=−1.

and

$$\tau_r = \left[\mu\left(\frac{\partial u}{\partial z}+\frac{\partial w}{\partial r}\right)\right]_{z=0} = \mu_0(1+)^a R_e^{\frac{1}{2}}\Omega F'(0).$$

Hence the tangential and radial skin frictions are respectively given by

$$(1+\varepsilon)^{-a}R_e^{\frac{1}{2}}C_{f_t} = G'(0), \tag{17}$$

and

$$(1+\varepsilon)^{-a}R_e^{\frac{1}{2}}C_{f_r} = F'(0). \tag{18}$$

Fourier's law

$$q = -\left(\kappa\frac{\partial T}{\partial z}\right)_{z=0} = -\kappa_0\Delta T(1+\varepsilon)^b\left(\frac{\Omega}{\nu_0}\right)^{\frac{1}{2}}\theta'(0), \tag{19}$$

is used to calculate the rate of heat transfer from the disk surface to the fluid. The Nusselt number Nu is obtained as

$$(1+\varepsilon)^{-b}R_e^{\frac{1}{2}}Nu = -\theta'(0), \tag{20}$$

where Re ($=\Omega r^2/\nu_0$) is the rotational Reynolds number.

4. Method of solution

Eqs. (11)–(16) are solved numerically using a shooting method for different values of suction $W<0$ and parameters Pr, Ec, β_e, β_i, δ, M and ε. To reduce the equations to first order equations we set $F=y_1$, $G=y_2$, $H=y_3$, $\theta=y_4$, $F'=y_5$, $G'=y_6$, $\theta'=y_7$ to get;

$$
\begin{aligned}
y_1' &= y_5, y_1(0) = \gamma s^{(5)} \\
y_2' &= y_6, y_2(0) = 1 + \gamma s^{(6)}, \\
y_3' &= -2y_1 - cy_3y_7(1+\varepsilon y_4)^{-1}\varepsilon, y_3(0) = W, \\
y_4' &= y_7, y_4(0) = 1, \\
y_5' &= -a\varepsilon y_5 y_7(1+\varepsilon y_4)^{-1} + \left[\frac{\delta\eta}{2}y_5 + \delta y_1 + y_1^2 + y_2^2 = y_3 y_5\right](1+\varepsilon y_4)^{c-a} \\
&\quad + \left[\frac{M(\alpha y_1 = \beta_e y_2)}{\alpha^2+\beta_e^2}\right](1+\varepsilon y_4)^{-a}, y_5(0) = s^{(5)}, \\
y_6' &= -a\varepsilon y_7 y_6(1+\varepsilon y_4)^{-1} + \left[\frac{\delta\eta}{2}y_6 + \delta y_2 + 2y_1y_2 + y_3y_6\right](1+\varepsilon y_4)^{c-a} \\
&\quad + \left[\frac{M(\alpha y_2 - \beta_e y_1)}{\alpha^2+\beta_e^2}\right](1+\varepsilon y_4)^{-a}, y_6(0) = s^{(6)}, \\
y_7' &= -b\varepsilon y_7^2(1+\varepsilon y_4)^{-1} + Pr(1+\varepsilon y_4)^{-b}\left[\frac{\delta\eta}{2}y_7 + y_3y_7(1+\varepsilon y_4)^{-c}\right. \\
&\quad \left. + \frac{EcM\left(y_1^2+y_2^2\right)}{\alpha^2+\beta_e^2} + Ec\left(y_5^2+y_6^2\right)(1+\varepsilon y_4)^{a}\right], y_7(0) = s^{(7)},
\end{aligned}
\tag{21}
$$

where $s^{(5)}$, $s^{(6)}$ and $s^{(7)}$ are determined such that $y_5(\infty)=0$, $y_6(\infty)=0$ and $y_7(\infty)=0$. The essence of this method is to reduce the boundary value problem to an initial value problem and then use a shooting numerical techniques to guess

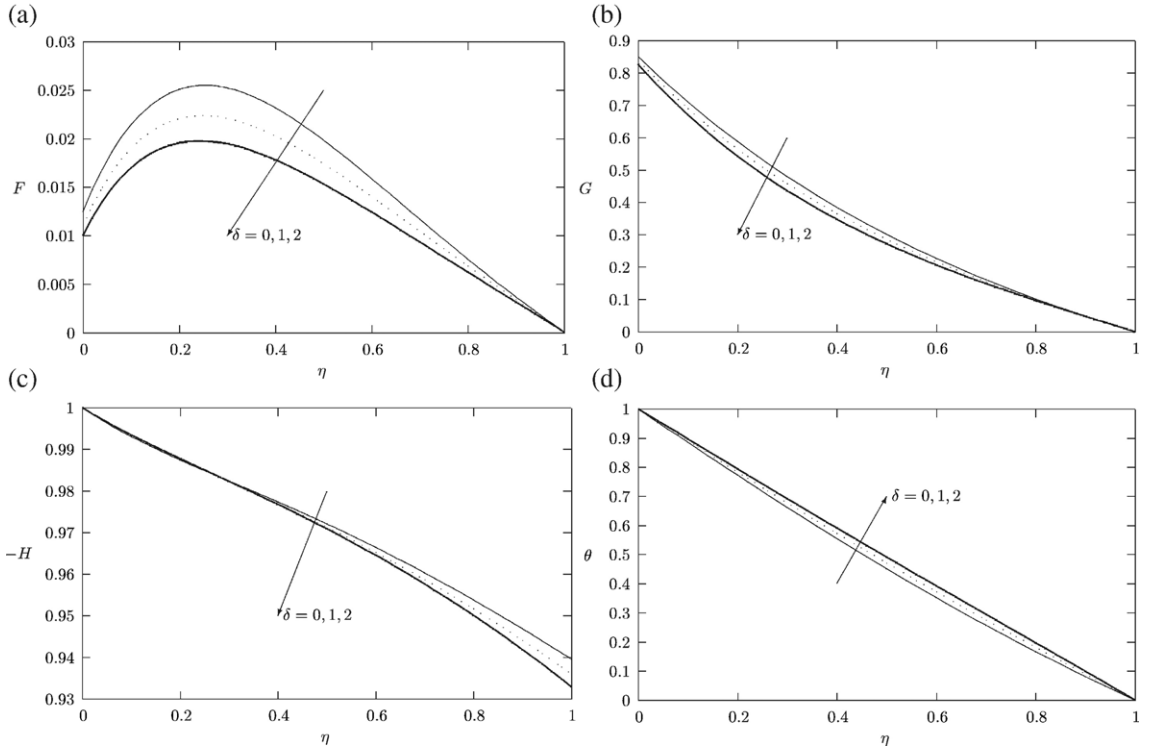

Fig. 3. (a) Effect of δ on the radial velocity profiles and (b) effect of δ on the tangential velocity profiles: for $Ec=0.3$, $Pr=0.72$, $\varepsilon=0.1$, $\beta_e=0.1$, $\beta_i=0.2$, $M=1$, $\gamma=0.1$ and $W=-1$. (c) Effect of δ on the axial velocity profiles and (d) effect of δ on the temperature profiles: for $Ec=0.3$, $Pr=0.72$, $\beta_e=0.1$, $\beta_i=0.2$, $M=1$, $\gamma=0.1$ and $W=-1$.

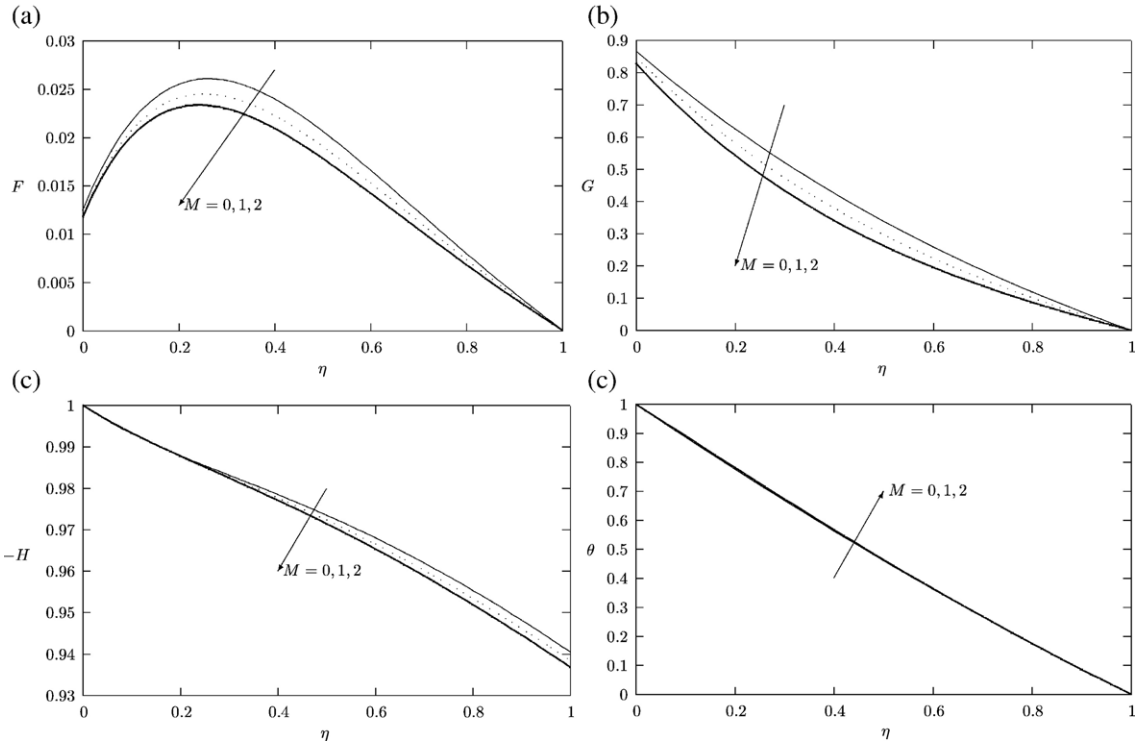

Fig. 4. (a) Effect of M on the radial velocity profiles and (b) effect of M on the tangential velocity profiles: for Ec=0.3, Pr=0.72, ε=0.1, β_e=0.1, β_i=0.2, δ=0.3, γ=0.1 and W=−1. (c) Effect of M on the axial velocity profiles and (d) effect of M on the temperature profiles: for Ec=0.3, Pr=0.72, ε=0.1, β_e=0.1, β_i=0.2, δ=0.3, γ=0.1 and W=−1.

$s^{(5)}$, $s^{(6)}$ and $s^{(7)}$ until the boundary conditions $y_5(\infty)=0$, $y_6(\infty)=0$ and $y_7(\infty)=0$ are satisfied. The resulting differential equations are then can be easily integrated using initial value solver, *lsode* and *fsolve* available in *GNU Octave*. It may be remarked that the steady-state Eqs. (11)–(16) in the absence of all of the constant property ($\varepsilon=0$), slip factor ($\gamma=0$), magnetic parameter ($M=0$), unsteadiness parameter ($\delta=0$), and Eckert number ($Ec=0$) are identical to those of Osalusi and Sibanda [12] and Maleque and Sattar [20], and a comparison of our numerical results is shown in Table 1. The three set of results compare favourable for $W<0$, hence an encouragement for the use of the present numerical computations.

5. Numerical results and discussion

For numerical computations, we took Pr=0.72, which is the value of Prandtl number for air. We have confined our analysis to the case when we have suction velocity only, that is, when $W<0$. Table 2 displays the numerical results for $F'(0)$, $-G'(0)$ and $-\theta'(0)$ for different values of γ, δ, M, Ec, β_e and β_i.

Inspection of Table 2 reveals that a moderate increase in the value of the slip factor γ may lead to a gradual monotonic decrease in the radial $F'(0)$ and tangential $-G'(0)$ skin-friction coefficient, while it increases the rate of heat transfer $-\theta'(0)$ coefficient. We also observe that an increase in the value of unsteadiness parameter δ may lead to a gradual monotonic decrease in the radial skin friction $F'(0)$ and rate of heat transfer $-\theta'(0)$, while it increases the tangential skin friction $-G'(0)$ coefficient. In Table 2 we notice that as M increases the shear stress in radial $F'(0)$ direction and the rate of heat transfer $-\theta'(0)$ decrease, while it increases the shear stress in tangential $-G'(0)$ direction. The reason for this trend is that the magnetic field reduces the radial and axial velocities, but increases the tangential velocity. Consequently, a monotonic decrease in the rate of heat transfer is due to heat created by both viscous dissipation and compression work ($Ec\neq0$). Further, we observe that radial skin friction $F'(0)$ and the rate of heat transfer $-\theta'(0)$ decreases with Ec while it increases $-G'(0)$. It is noted in Table 2 that negative heat transfer rates are obtained for some value of Ec (e.g. −0.25424283684431, −0.76712806748436). Negative values of $\theta'(0)$ indicate that heat is transfer from the fluid to the disk in spite of the excess of the surface temperature over that of the free stream fluid. This phenomenon can be explained as a fluid particle heated to nearly the wall temperature being convected downstream to a location where the wall temperature is lower. Also, increase

in the values of Hall parameter β_e increases both the shear stress in the radial $F'(0)$ direction and the rate of heat transfer $-\theta'(0)$ coefficient while increase in the value of β_e decreases shear stress in the tangential $-G'(0)$ direction. We observe from Table 2 that as ion-slip parameter β_i increases, the shear stress in radial skin friction $F'(0)$ and tangential skin friction $-G'(0)$ decrease and increases the rate of heat transfer $-\theta'(0)$.

Similarity solutions for three velocity components (radial, tangential and axial) and the temperature are presented in Fig. 2(a)–(d) for values of the slip coefficient γ in the range of 0.00 to 0.20. The shear-driven flow (G) in the tangential direction in Fig. 2(b) is gradually reduced with increasing values of γ. The centrifugal force associated with this circular motion causes the outward radial flow (F), which is correspondingly reduced with decreasing slip coefficient close to the disk surface. The radial outflow F is compensated by an axial inflow H towards the rotating disk, in accordance with the mass conservation equation (11) (i.e. when $\varepsilon=0$).

The gradual reduction of the peak in the F-profiles in Fig. 2(a) with decreasing values of γ is reflected in the distributions of the axial velocity component in Fig. 2(c). The distinct inflection point in the H-profiles for the highest values of γ seems to gradually disappear with increasing slip. This is a consequence of the direct coupling between the radial and axial velocity components through the continuity constraint [11]. The reduction of the radial velocity $F(\eta)$ with decreasing γ automatically gives rise to a reduced axial inflow (for constant property i.e. $\epsilon=0$) since

$$-H(\infty) = 2\int_0^\infty F \cdot d\eta. \tag{22}$$

Fig. 2(d) shows the temperature profile. A general decrease in temperature profile is observed with maximum at the disk surface and minimum far away from the disk. The magnitude of the temperature profiles decreases slightly with an increase in slip coefficient.

The effect of unsteadiness parameter δ with the numerical values of 0.0,1.0 and 2 is observed on the radial, tangential and axial velocity profiles F, G, $-H$ and on the temperature profile θ for $0\le\eta\le1$ and $Pr=0.72$ as presented in Fig. 3(a)–(d). From these figures it is evident that the radial velocity F, tangential velocity G and axial velocity $-H$, decrease everywhere as δ increases, but an increase in temperature profiles, θ, is observed. Fig. 4(a)–(d) shows typical profiles for the fluid radial velocity F, tangential velocity G, axial velocity $-H$ and temperature θ for different values of the magnetic parameter M, respectively. Due to the damping effect of

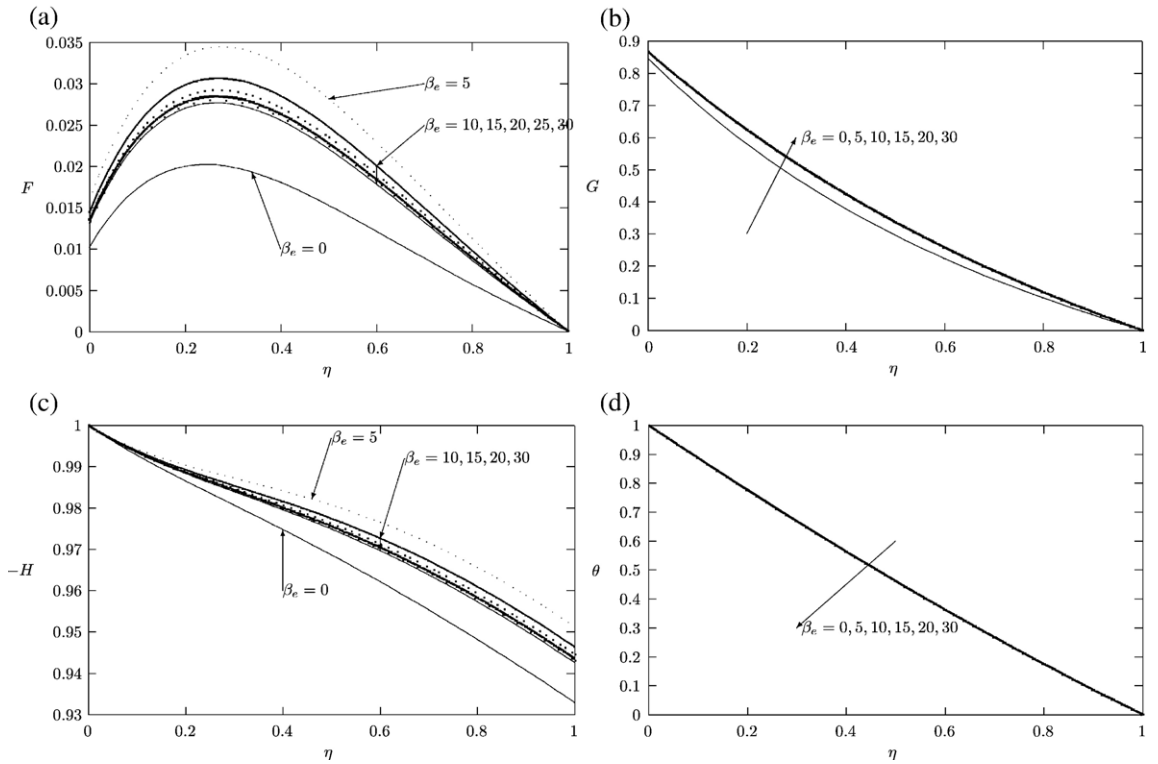

Fig. 5. (a) Effect of β_e on the radial velocity profiles, (b) effect of β_e on the tangential velocity profiles: for $Ec=0.3$, $Pr=0.72$, $\varepsilon=0.1$, $\beta_i=0.2$, $M=1$, $\gamma=0.1$ and $W=-1$. (c) Effect of β_e on the axial velocity profiles and (d) effect of β_e on the temperature profiles: for $Ec=0.3$, $Pr=0.72$, $\varepsilon=0.1$, $\beta_i=0.2$, $\delta=0.3$, $M=1$, $\gamma=0.1$ and $W=-1$.

the magnetic field, increases in the values of M have a tendency to slow the motion of the fluid in radial F, tangential G and axial $-H$ directions and make it warmer as it moves over the disk causing the temperature θ to increase. Fig. 5(a)–(d) shows the F, G, $-H$ and θ profiles for various values of β_e of 0, 5, 10, 15, 20, 25 and 30. We observe that radial velocity F, tangential velocity G and axial velocity $-H$ increase while the temperature θ decreases as the Hall current parameter β_e increases since the magnetic damping on F, G and $-H$ decrease as β_e increase and the magnetic field has a propelling effect on F, G and $-H$. Also it is shown that the F, G, $-H$ and θ profiles approach their classical values when the Hall parameter β_e increases to ∞ since the magnetic force terms approach zero values for very large values of β_e. On the other hand, Fig. 5(a) and (c) shows the radial flow F (and hence the axial flow $-H$ (Eq. (10))), begins to develop as the Hall parameter β_e increases from zero, forms a maximum profile for $\beta_e = 5$ and decreases for $\beta_e > 5$ being equal to zero when β_e becomes very large.

Fig. 6(a)–(d) describes the behaviour of F, G and θ with changes in the values of the ion-slip parameter β_i. From Fig. 6(a), (c) and (d) it is clear that an increase in the ion-slip parameter β_i leads to a decrease in the radial velocity F, axial velocity $-H$ and temperature θ. In Fig. 5(b) we observe that the effect of increasing the ion-slip parameter β_i is to decrease G. In general, it is noted that, the effect of Hall parameter β_e on the flow and thermal fields is more notable than that of ion-slip parameter β_i. This is due to the fact that the diffusion velocity of the electrons is much larger than that of ions. Fig. 7(a)–(d) illustrates the radial velocity F, tangential velocity G, axial velocity $-H$ and temperature θ profiles for various values of Ec of 0, 1, and 2. From Fig. 7(b)–(d) we may conclude that the presence of viscous dissipation and Ohmic heating is to increase the tangential velocity G, axial velocity $-H$ and temperature θ while Ec decreases the radial velocity. The rise in the temperature θ is due to the heat created by viscous dissipation and compression work ($Ec = 0$). This behaviour is shown in Fig. 7(d).

6. Conclusions

In this study we have examined the effect of Ohmic heating and viscous dissipation on unsteady hydro-magnetic and slip flow of a viscous fluid over a porous rotating disk in the presence of Hall and ion-slip currents taking into account the variable properties of the fluid. The time-dependent angular velocity was taken to vary inversely as a linear function

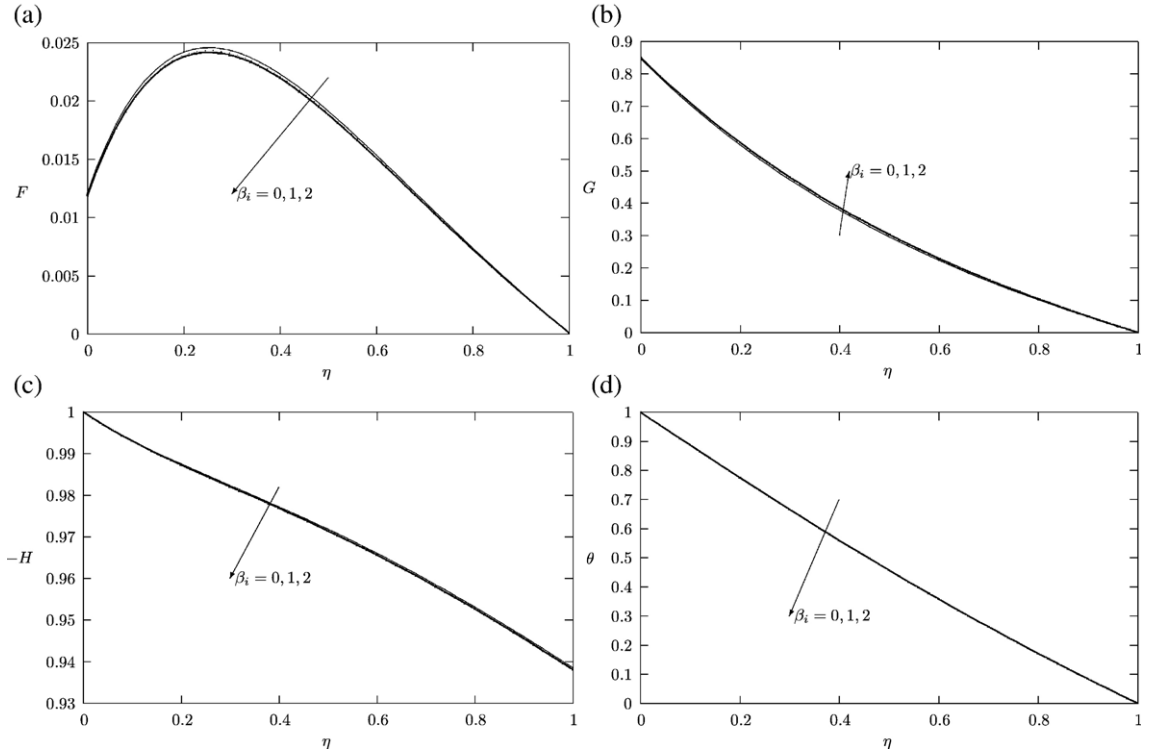

Fig. 6. (a) Effect of β_i on the radial velocity profiles, (b) effect of β_i on the tangential velocity profiles: for $Ec = 0.3$, $Pr = 0.72$, $\varepsilon = 0.1$, $\beta_e = 0.1$, $\delta = 0.3$, $M = 1$, $\gamma = 0.1$ and $W = -1$. (c) Effect of β_i on the axial velocity profiles and (d) effect of β_i on the temperature profiles: for $Ec = 0.3$, $Pr = 0.72$, $\varepsilon = 0.1$, $\beta_e = 0.1$, $\delta = 0.3$, $M = 1$, $\gamma = 0.1$ and $W = -1$.

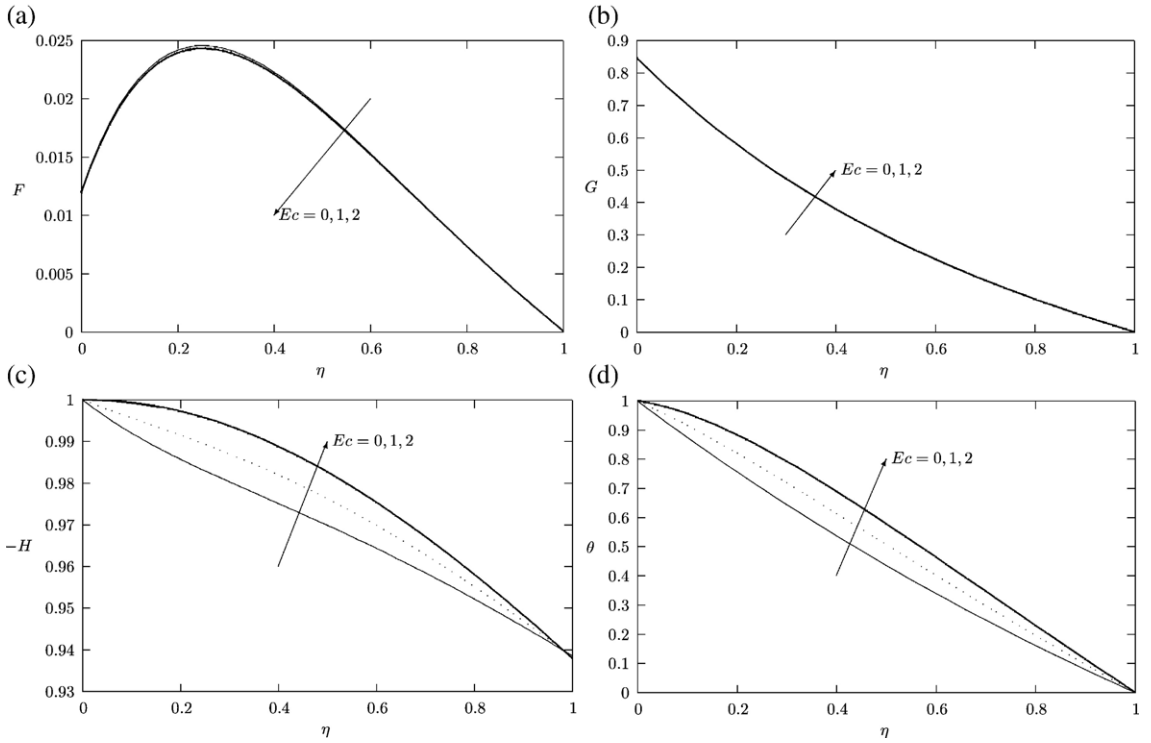

Fig. 7. (a) Effect of *Ec* on the radial velocity profiles, (b) effect of *Ec* on the tangential velocity profiles: for $Pr=0.72$, $\varepsilon=0.1$, $\beta_e=0.1$, $\beta_i=0.2$, $\delta=0.3$, $M=1$, $\gamma=0.1$ and $W=-1$. (c) Effect of *Ec* on the axial velocity profiles and (d) effect of *Ec* on the temperature profiles: for $Pr=0.72$, $\varepsilon=0.1$, $\beta_e=0.1$, $\beta_i=0.2$, $\delta=0.3$, $M=1$, $\gamma=0.1$ and $W=-1$.

of time. Employing von Karman similarity transformation technique, the governing equations are transformed into ordinary differential equations and solve numerically by a shooting method. We present results to illustrate the flow characteristics for the velocity and temperature fields as well as the skin friction and rate of heat transfer, and show how the flow fields are influenced by the material parameters of the flow problem. We can conclude from our results that both the slip factor and unsteadiness parameter affect the velocity as well as skin friction likewise the temperature as well as the rate of heat transfer. We noticed that the increase in slip and unsteadiness parameters is accompanied by a decrease in radial skin-friction coefficient and rate of heat transfer. We also discovered that an increase in unsteadiness parameter decreases the velocity of the fluid and increases the temperature. Increase in Hall parameter β_e, ion-slip parameter β_i decreases the temperature profiles while the temperature increases with an increase in both magnetic parameter M and Eckert number *Ec*.

Acknowledgement

This work is based upon work funded by TOTAL E&P (UK) for PhD studentship research in Marine Renewable Energy in the Institute of Petroleum Engineering, Heriot-Watt University, UK.

References

[1] T. von Karman, Uber laminare und turbulente Reibung, Z. Angew. Math. Mech. 1 (1921) 233–255 (1921).
[2] W.G. Cochran, The flow due to a rotating disk, Proc. Camb. Philos. Soc. 30 (3) (1934) 365–375.
[3] E.R. Benton, On the flow due to a rotating disk, J. Fluid Mech. 24 (1966) 781–800.
[4] P. Mitschka, Nicht-Newtonsche Flussigkeiten. II. Drehstomungen Ostwarld-deWaelescher Nicht-Newtonscher Flus-sigkeiten, Coll. Czech., Chem. Comm. 29 (1964) 2892–2905.
[5] A. Arikoglu, I. Ozkol, On the MHD and slip flow over a rotating disk with heat transfer, Int. J. Numer Methods Heat Fluid Flow 28 (2) (2006) 172–184.

[6] T.M.A. El-Mistikawy, H.A. Attia, A.A. Megahed, The rotating disk flow in the presence of a weak magnetic field, Proc. 4th Conf. on Theoret. and Appl. Mech., Cairo, Egypt, November 5–7, 1990, pp. 69–82.
[7] E.M.A. Elbashbeshy, M.F. Dimian, Effect of radiation on the flow and heat transfer over a wedge with variable viscosity, Appl. Math. Comput. 132 (2002) 445–454.
[8] H.A. Attia, A.L. Aboul-Hassan, On hydromagnetic flow due to a rotating disk, Appl. Math. Model. 28 (2004) 1007–1014.
[9] H.A. Attia, Unsteady flow and heat transfer of viscous incompressible fluid with temperature-dependent viscosity due to a rotating disc in a porous medium, J. Phys. A, Math. Gen. 39 (2006) 979–991.
[10] E.M. Sparrow, G.S. Beavers, L.Y. Hung, Flow about a porous-surface rotating disk, Int. J. Heat Mas Tranfer 14 (1971) 993–996.
[11] M. Miklavcic, C.Y. Wang, The flow due to a rough rotating disk, Z. Angew. Math. Phys. 55 (2004) 235–246.
[12] E. Osalusi, P. Sibanda, On variable laminar convective flow properties due to a porous rotating disk in a magnetic field, Rom. J. Phys. 51 (2006) Nos. 9–10, 933–944.
[13] M.G. Rogers, G.N. Lance, The rotationally symmetric flow of a viscous fluid in presence of infinite rotating disk, J. Fluid Mech. 7 (1960) 617–631.
[14] P.J. Zandbergen, D. Dijksra, Von Karman swirling flows, Ann. Rev. Fluid Mech. 19 (1987) 465–491.
[15] J.M. Owen, R.H. Rogers, Flow and Heat Transfer in Rotating Disk Systems Rotor-Stator Systems, vol. 1, Research Study Press (John Wiley), Taunton, 1989.
[16] H.I. Andersson, E. de Korte, O.A. Meland, Flow of a power-law fluid over a rotating disk revisited, Fluid Dyn. Res. 28 (2001) 75–88.
[17] J.P. Denier, R.E. Hewitt, Asymptotic matching constraints for a boundary-layer flow of power-law fluid, J. Fluid Mech. 518 (2004) 261–279.
[18] H. Herwig, The effect of variable properties on momentum and heat transfer in a tube with constant heat flux across the wall, Int. J. Heat Mass Transfer 28 (1985) 424–441.
[19] H. Herwig, K. Klemp, Variable property effects of fully developed laminar flow in concentric annuli, ASME J. Heat Transfer 110 (1988) 314–320.
[20] A.K. Maleque, A.M. Sattar, Steady laminar convective flow with variable properties due to a porous rotating disk, J. Heat Transfer 127 (2005) 1406–1409.
[21] J.T. Stuart, On the effect of uniform suction on the steady flow due to a rotating disk, Q. J. Mech. Appl. Math. 7 (1954) 446–457.
[22] M.M. Ali, T.S. Chen, B.F. Armaly, Natural convection–radiation interaction in boundary-layer flow over horizontal surfaces, AIAA J. 22 (1984) 1797–1803.
[23] A.R. Bestman, S.K. Adjepong, Unsteady hydromagnetic free-convection flow with radiative heat transfer in a rotating fluid, Astrophys. Space Sci. 143 (1988) 73–80.
[24] E.M.A. Elbashbeshy, M.F. Dimian, Effect of radiation on the flow and heat transfer over a wedge with variable viscosity, Appl. Math. Comput. 132 (2002) 445–454.
[25] M. Gad-el-Hak, The fluid mechanics of microdevices—the free scholar lecture, J. Fluid Eng-T. Asme vol. 121 (1999) 5–33.
[26] J. Herrero, J.A.C. Humphrey, F. Gilralt, Comparative analysis of coupled flow and heat transfer between co-rotating disks in rotating and fixed cylindrical enclosures, ASME J. Heat Transfer 300 (1994) 111–121.
[27] M.A. Hossain, M.A. Alim, D. Rees, The effect of radiation on free convection from porous vertical plate, Int. J. Heat Mass Transfer 42 (1999) 181–191.
[28] M.A. Hossain, K. Khanafer, K. Vafai, The effect of radiation on free convection of fluid with variable viscosity from a porous vertical plate, Int. J. Therm. Sci. 40 (2001) 115–124.
[29] F.S. Ibrahim, Mixed convection–radiation interaction in boundary-layer flow over horizontal surfaces, Astrophys. Space Sci. 168 (1990) 263–276.
[30] S. Jayaraj, Thermophoresis in laminar flow over cold inclined plates with variable properties, Heat Mass Transfer 40 (1995) 167–174.
[31] N. Kelson, A. Desseaux, Note on porous rotating disk flow, Anziam J. 42 (2000) C847–C855 (E).
[32] M.A. Mansour, Radiative and free-convection effects on the oscillatory flow past a vertical plate, Astrophys. Space Sci. 166 (1990) 269–275.
[33] A. Raptis, C. Perdikis, H.S. Takhar, Effect of thermal radiation on MHD flow, Appl. Math. Comput. 153 (2004) 645–649.
[34] H.S. Takhar, R. Gorla, V.M. Soundalgekar, Radiation effects on MHD free convection flow of gas past a semi-infinite vertical plate, Int. J. Numer. Methods Heat Fluid Flow 6 (1996) 77–83.
[35] A.J. Chamkha, Mixed convection flow along a vertical permeable plate embedded in a porous medium in the presence of a transverse magnetic field, Numer. Heat Transf., Part A Appl. 34 (1998) 93–103.
[36] T.K. Aldoss, Y.D. Ali, M.A. Al-Nimr, MHD mixed convection from a horizontal circular cylinder, Numer. Heat Transf., Part A Appl. 30 (1996) 379–396.
[37] M. Molki, M.K. Nagalla, Flow characteristics of rotating disks simulating a computer hard drive, Numer. Heat Transf., Part A Appl. 48 (8) (2005) 745–761.
[38] P. Sandilya, G. Biswas, G. Rao, A. Sharma, Numerical simulation of the gas flow and mass transfer between two coaxially rotating disks, Numer. Heat Transf., Part A Appl. 39 (3) (2001) 285–305.
[39] J.S. Yoo, Unsteady heat transfer from a rotating disk with solidification, Numer. Heat Transf., Part A Appl. 31 (7) (1997) 765–781.
[40] J.W. Wu, H.J. Rath, Finite-difference method of incompressible flows with rotation and moving boundary in a nonstaggered grid, Numer. Heat Transf., Part B Fund. 26 (2) (1994) 189–206.